Engineered Science
DOI: https://dx.doi.org/10.30919/es8e816

Mildew-resistant Wood Building Materials with Titanium Oxide Nanosheet

Haiquan Zhang,[1,#] Shuliang Li,[2,#] Huancheng Hang,[3,#] Renjuan Wang,[1] Changjing Cheng,[3] Kuzin Victor Fedorovich[4] and Xianmin Mai[2,*]

Abstract

The wood is an ideal green building material because of its high strength-to-weight ratio, renewable nature, and excellent heat insulation/noise reduction/humidity control performances. However, rich nutrients make wood materials easy to microbial erosion, which limits application in the construction field. Herein, a novel anti-mildew technology is reported, which fills titanium oxide ($Ti_{0.87}O_2$) nanosheet into the open pores of wood materials spontaneously. Based on the high light transmittance of $Ti_{0.87}O_2$ nanosheet, the as-prepared composite wood retains the original texture and color of wood. There are multiple coordination bonds between the hydroxyl of cellulose/lignin and Ti^{4+} of titanium oxide, which enhances the stability of the interface between the wood material and $Ti_{0.87}O_2$ nanosheet. The $Ti_{0.87}O_2$ filling medium cuts off the transmission path of oxygen, water, nutrients and microorganisms, making the composite wood have good mildew resistance. Therefore, the modification technology makes wood have great application potential in the field of structure and decoration.

Keywords: Wood building material; Titanium oxide nanosheet; Natural texture; Coordination bond; Mildew resistance.
Received: 30 December 2022; Revised: 13 January 2022; Accepted: 05 February 2023.
Article type: Research article.

1. Introduction

As a renewable bio-based resource, wood materials have been attracting more and more interests.[1-5] However, biological pathogens such as fungi, bacteria and mildew are susceptible to infect wood materials, resulting in the failure of wood color[6-9] and mechanical properties.[10-12] Mildew such as Trichoderma species have been reported to produce an enzyme that hydrolyzes cellulose into glucose.[13] Prolonged exposure to mildewy wood can cause allergies, respiratory inflammation and mucosal disease.[14-16] Various anti-mildew agents have been developed, such as chromated copper arsenate (CCA), ammoniacal copper quat (ACQ) and chitosan-copper complex (CCC).[17-23] These traditional wood preservatives have been limited in commercial application due to strong toxicity, easy diffusion, and difficult degradation.

It is of great importance to develop environment-friendly high-performance wood preservatives. Wood preservatives represented by nano bactericides have the advantages of photocatalysis and anti-bacterial properties.[24,25] For example, pine wood samples impregnated with 1–5 wt% zinc oxide (ZnO) nanorods[26] showed decay resistance against the growth of white-rot fungus. Among nano-scale anti-mildew agents, titanium dioxide (TiO_2) has been accepted as one of the most effective anti-microbial agents,[27,28] decomposing microorganisms into carbon dioxide and water by means of photocatalysis.[29,30] Anti-fungal activity against the growth of white rot fungus (Ganoderma applanatum, Hypocrealixii) and brown rot fungi (Mucor circineloides) has been confirmed in various woods treated with TiO_2.[31,32] However, it is difficult for TiO_2 nanoparticles to penetrate into the pores of wood due to the lack of a dispersion mechanism. In addition, white TiO_2 nanocoating masks the natural texture and color of wood material.

[1] *State Key Laboratory of Marine Resource Utilization in South China Sea, Hainan University Haikou 570228, P.R. China*
[2] *School of Architecture, Southwest Minzu University, Chengdu 610041, P. R. China*
[3] *School of Chemistry & Environment, Southwest Minzu University, Chengdu 610041, P. R.*
[4] *Section of Geology, Mining and Processing of Minerals, Russian Academy of Engineering, Moscow 125009, Russia*
[#] *These authors contributed equally to this work.*
**E-mail:* maixianmin@foxmail.com (X. Mai)

Layered materials such as graphite, oxides, metallic alloys, layered double hydroxides have been attracting much attention, which exhibit interesting properties owing to their two-dimensional (2D) nature.[33-38] In searching for an alternative to TiO_2 nanoparticles, we have focused on $Ti_{0.87}O_2$ nanosheet. Compared with other titania-based materials, the $Ti_{0.87}O_2$ nanosheet have some unique features.[39,40] The unilamellar $Ti_{0.87}O_2$ nanosheet are transparent, so that the treated wood would retain its natural color. $Ti_{0.87}O_2$ nanosheet is long-term stable in the suspension due to the existence of Ti vacancies and negatively charged properties. Due to the two-dimensional structure, $Ti_{0.87}O_2$ nanosheet has strong photocatalytic property in the UV range and provides more reacting points.

Herein, we employed a straightforward impregnation method to spontaneously infiltrate hyper-dispersed $Ti_{0.87}O_2$ nanosheet into the micropores of wood material, resulting in the as-prepared composite wood resistant to microbial corrosion. The coordination between the hydroxyl group of cellulose/lignin and Ti^{4+} of the $Ti_{0.87}O_2$ nanosheet significantly enhanced the interface contact between wood and titanium oxide. With the high dispersion of $Ti_{0.87}O_2$ nanosheet and the coordination with hydroxyl, titanium oxide nanomaterial is filled in the open pores of wood. The filling medium blocks the material exchange between the environment and wood material, and greatly enhances the mildew resistance of the wood. At the same time, the high light transmittance of $Ti_{0.87}O_2$ nanosheet keeps the original texture and color of the composite wood. Long-lasted mildew resistance makes wood composite as a building material have great potential in the future.

2. Experimental section

2.1. Material

All the experimental chemicals were of analytical grade and used without further purification. Hydrochloric acid (HCl, 37%) and tetrabutylammonium hydroxide (TBAOH, 40 wt% solution in methanol) were purchased from Sinopharm Chemical Reagent Co., Ltd. Potassium chloride (KCl, 99.5%), TiO_2 (99.5%) and Potassium carbonate (K_2CO_3, 99.5%) were purchased from Aladdin. Lithium carbonate (Li_2CO_3, 99.5%) was purchased from Shanghai Macklin Biochemical Co., Ltd. Wood blocks were obtained from Pinus Sylvestris (PS). All specimens were free of mildew, blue stains, and knots. The wood specimens for the anti-mildew activity test were processed into a shape of 6 mm × 6 mm × 6 mm.

2.2. Preparation

2.2.1 Synthesis of $Ti_{0.87}O_2$

Li_2CO_3, TiO_2 and K_2CO_3 were mixed with a molar ratio of 0.14:1.73:0.4 and then pre-calcined at 900 °C for 1 h,[41,42] as shown in Fig. 1. The mixture was subsequently ground and further calcinated 900 °C for 20 h. Layered titanate $K_{0.8}Ti_{1.73}Li_{0.27}O_4$ was produced and delaminated into molecular single sheets. Specifically, 4 g of the layered bulk precursor $K_{0.8}Ti_{1.73}Li_{0.27}O_4$ was steeped in 0.5 m L^{-1} HCl solution and stirred at ambient temperature for 7 days to perform acid exchange. The product was recovered by

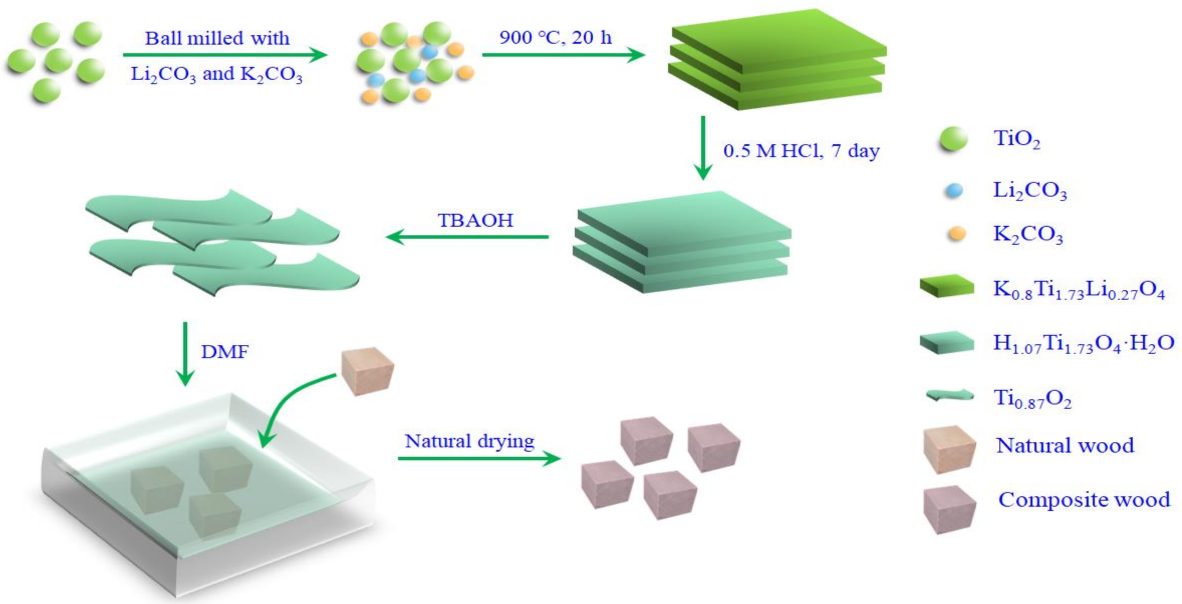

Fig. 1 Schematic illustration for the synthesis of the PS/$Ti_{0.87}O_2$ composite wood. **Note**: The proposed intercalation mechanism[39-42]. (a) The acid-base reaction starts with diffusion of OH^- from tetra-n-butylammo-nium hydroxide into $H_{1.07}Ti_{1.73}O_4{\cdot}H_2O$, followed by their reaction with protons; (b) The layered structure of HTO loses its stability because of the acid-base reaction; (c) Isolated nanosheet is thus obtained.

filtration, washed to neutral, and dried at room temperature. Subsequently, 1 g of the obtained protonated layered compound $H_{1.07}Ti_{1.73}O_4·H_2O$ (HTO) was added to 250 mL of TBAOH solution. Finally, the mixture was mechanically shaken by oscillator at a rotational speed of 150 r min^{-1} $Ti_{0.87}O_2$ nanosheet were obtained.

2.2.2 Preparation of $Ti_{0.87}O_2$ coatings

The wood pieces were first cleaned with deionized water and dried at 160 °C in a vacuum. The as-prepared wood pieces were immersed in dimethyl formamide dispersion containing $Ti_{0.87}O_2$ nanosheet for 36 h. Pinus Sylvestris composite after dimethyl form amide evaporation is named as PS/$Ti_{0.87}O_2$.

2.3 Characterizations

SEM (JEOL, JEM-2100F) was used to investigate the morphology of $Ti_{0.87}O_2$ nanosheet. The distributions and interface characteristics of $Ti_{0.87}O_2$ nanosheet in wood were observed by SEM coupled to an EDS. The chemical changes of the treated wood spices were characterized by FTIR spectroscopy (Thermo Scientific Nicolet iS5with KBr pellet). WCAs at ambient temperature were measured on a contact angle system (Chengde Youte Testing Instrument Manufacturing Co., Ltd.). Aspergillus niger was used in the anti-mildew activity study. Strains were cultured in potato dextrose broth at 27 °C till visible mycelia were observed. Potato dextrose agar (PDA) plates were prepared and inoculated with 7-day-old culture from the tested mildews. The $Ti_{0.87}O_2$ nanosheet treated wood samples were placed in the center of the plates and incubated at 27 °C for 5 days, after which time the clear inhibition zones formed around the treated wood was measured by a ruler.

3. Results and discussion

$Ti_{0.87}O_2$ nanosheet was synthesized by coupling high temperature calcination, proton substitution and chemical exfoliation techniques in Fig. 1. As shown in Fig. 2a, the as-prepared $Ti_{0.87}O_2$ sample with the size of 5–25 μm displays a classical two-dimensional nanostructure. The as-prepared $Ti_{0.87}O_2$, commercial TiO_2 and ZnO (~10 nm) powders were separately transferred into three small glass bottles respectively, and then were dispersed in dimethyl formamide (DMF) to form a relatively stable turbid suspension using ultra-sonication for 20 min. After being placed for 5 min, the TiO_2 and ZnO nanomaterials fully precipitated to the bottom of the glass bottle. However, the $Ti_{0.87}O_2$ nano-material still formed stable turbid suspension in Fig. 2c. The result reveals the self-dispersion of the as-prepared $Ti_{0.87}O_2$ nano-material.

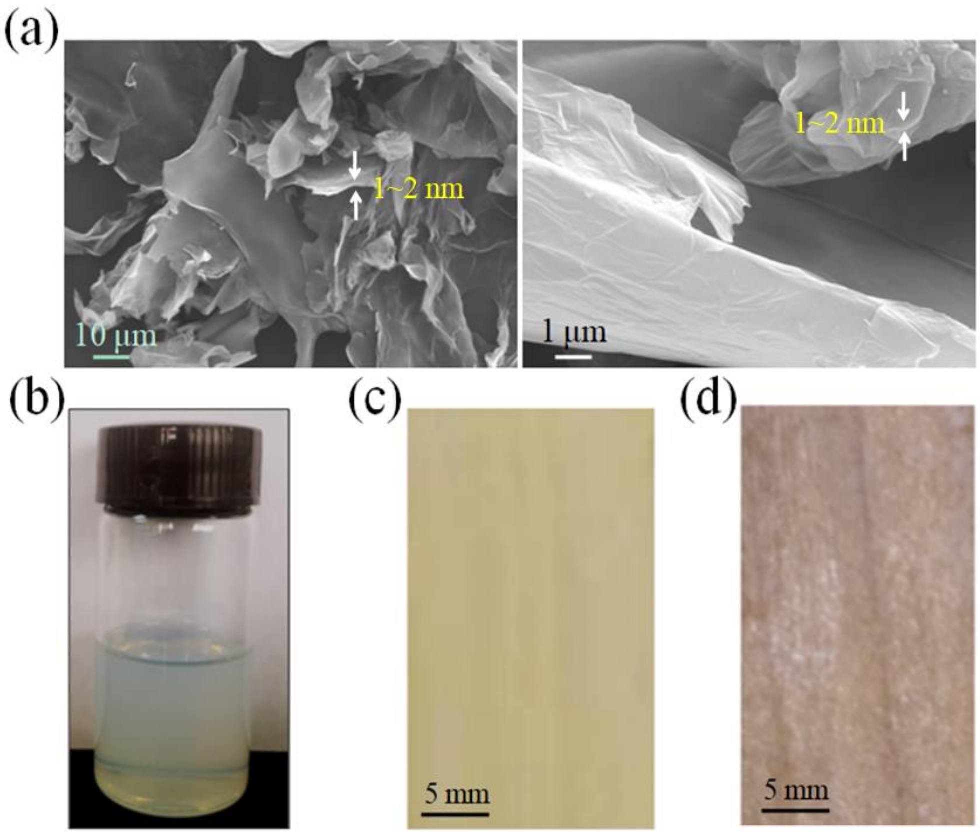

Fig. 2 Morphology of the as-prepared $Ti_{0.87}O_2$ nanomaterial. (a) SEM images; (b) $Ti_{0.87}O_2$ suspension (100 mg ml^{-1}) after being placed for 20 min; (c) Digital photo of the natural wood; (d) Digital photo of the PS/$Ti_{0.87}O_2$ composite.

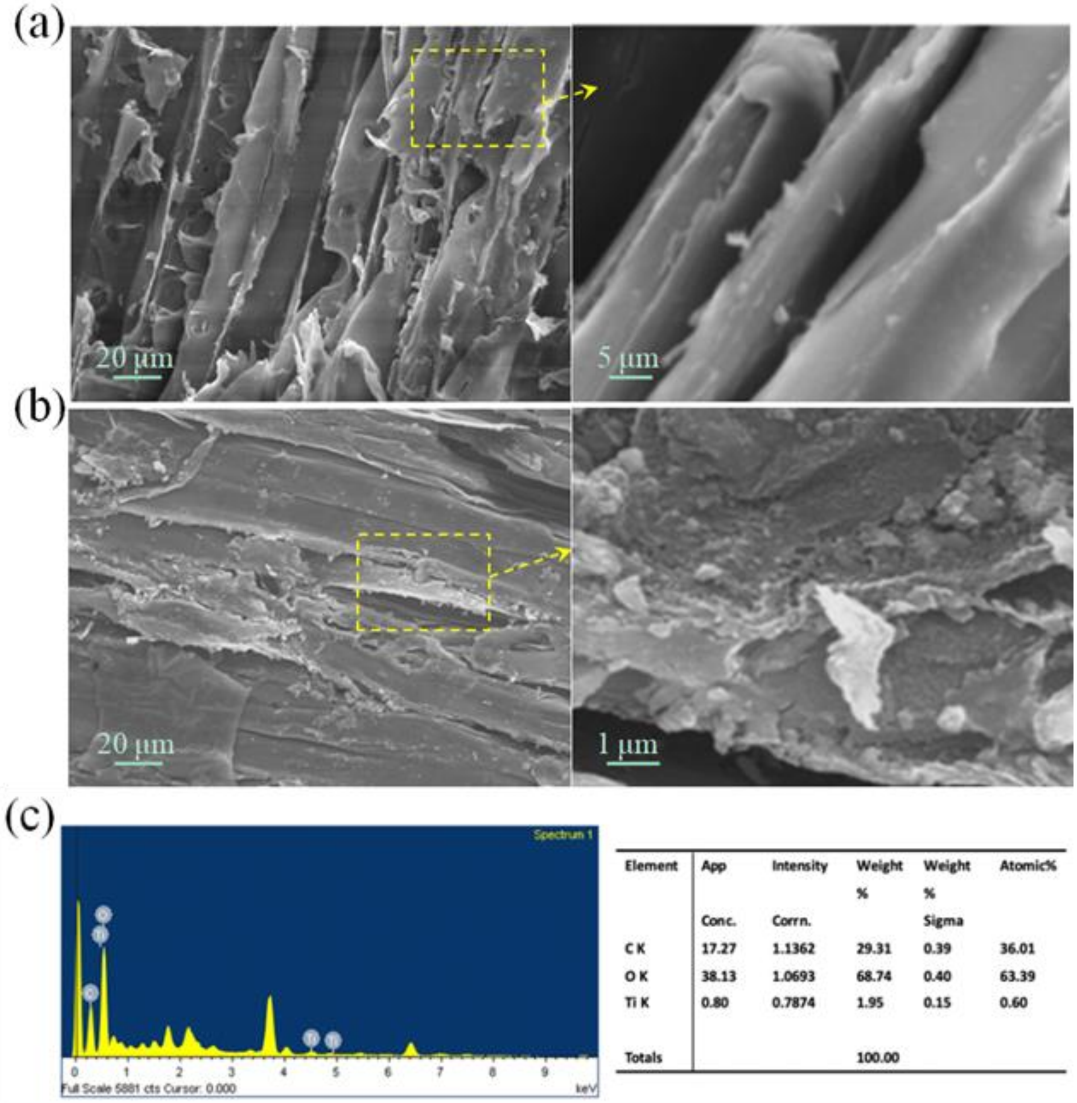

Element	App Conc.	Intensity Corrn.	Weight %	Weight % Sigma	Atomic%
C K	17.27	1.1362	29.31	0.39	36.01
O K	38.13	1.0693	68.74	0.40	63.39
Ti K	0.80	0.7874	1.95	0.15	0.60
Totals			100.00		

Fig. 3 Micromorphology of the PS/$Ti_{0.87}O_2$ composite wood. (a) Natural wood; (b) PS/$Ti_{0.87}O_2$; (c) EDS data of the PS/$Ti_{0.87}O_2$.

Different from the traditional coating technology, the penetration method has at least two advantages: (1) Under the same loading rate of titanium oxide, the color and texture of the composite wood prepared by the penetration method are closer to the natural wood; (2) The infiltration method increases the contact area/force between titanium oxide and wood, and significantly improves the interface stability.

The PS/$Ti_{0.87}O_2$ composite wood was prepared using a straightforward impregnation method in Fig. 1. Based on the high light transmittance of $Ti_{0.87}O_2$ nano-material (Fig. 2b), the PS/$Ti_{0.87}O_2$ composite wood shows the color and texture similar to the natural PS wood in Fig. 2d. Compared with natural PS wood, a large number of $Ti_{0.87}O_2$ nanosheets were observed in the conduits and cavities of the PS/$Ti_{0.87}O_2$ composite wood (Fig. 3b). EDS results further confirmed that the nanosheet spontaneously infiltrated into PS wood matrix in Fig. 3c.

To understand the combination rule between $Ti_{0.87}O_2$ nanosheet and wood, FT-IR spectra were carried out in Fig. S1. A new characteristic absorption peak was observed at the wave number of 669 cm^{-1} for the PS/$Ti_{0.87}O_2$ composite wood, which belongs to Ti-O-Ti bond.[43] The vibration absorption peaks of the cellulose/lignin hydroxyl (-OH, 3412 cm^{-1}), carbonyl (C=O, 1033 cm^{-1}) and phenolic hydroxyl (-OH, 1226 cm^{-1}) was weakened for the PS/$Ti_{0.87}O_2$ composite wood, indicating that there were coordination between hydroxyl, carbonyl and Ti^{4+}. Therefore, the $Ti_{0.87}O_2$ nanosheet can spontaneously diffuse and deposit into the open pores of the wood material. On the other hand, $Ti_{0.87}O_2$ nanosheet increased the roughness of wood at the micro-scale. The contact angle the PS/$Ti_{0.87}O_2$ composite wood increased from 39.1° of the natural PS wood to 65.6° in Fig. S2.

Figure 4 shows the mildew resistance of the PS wood loaded with the $Ti_{0.87}O_2$ nanosheet to typical Aspergillus niger. It is well known that natural PS wood has no antibacterial properties. However, we observed a bacteriostatic ring with a diameter of about 37 mm on the surface of composite wood, even if it was not exposed to ultraviolet or visible light. Mildew growth is an extremely complex process, which depends on appropriate temperature, humidity, oxygen, pH, nutrients and mineral elements. It is reasonable to speculate that the $Ti_{0.87}O_2$ nano-material filled in the open pores can cut off the water source and prevent the spread of mildew to the wood matrix. Therefore, the well-designed PS/$Ti_{0.87}O_2$ composite wood shows excellent mildew resistance even without relying on the photocatalytic effect.

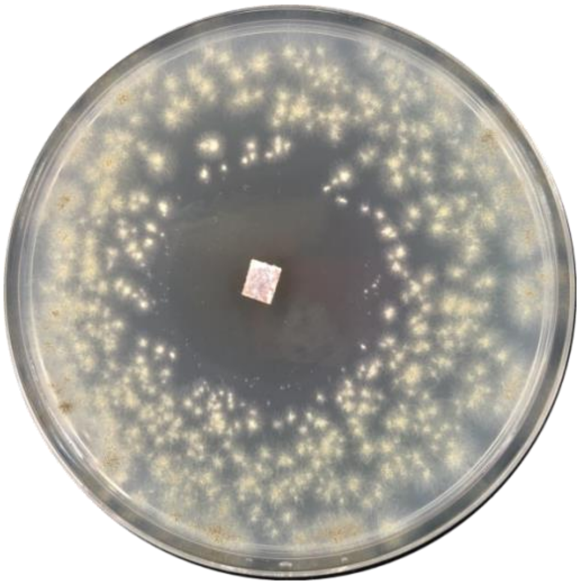

Fig. 4 Bacteriostatic ring of the PS/$Ti_{0.87}O_2$ composite wood. Note: *Aspergillus niger* was used as a target and cultured at 27 °C for 5 days.

4. Conclusions

As a classical building material, wood is easily corroded by microorganisms in humid environment, resulting in the failure of its color and mechanical properties. We have carefully designed an anti-mildew technology by introducing entropy-driven $Ti_{0.87}O_2$ nanosheet to the open pores of the wood. As-prepared $Ti_{0.87}O_2$ nanosheet is firmly fixed in the micro/nano-scale pores of the wood material, due to cross-linking between the electron withdrawing groups (hydroxyl, phenolic hydroxyl and carbonyl) of cellulose/lignin and Ti^{4+} of the $Ti_{0.87}O_2$ filling medium. This unique combination mode cuts off the mass transfer channel of water, oxygen and microorganism in the air to the wood material. Therefore, the PS/$Ti_{0.87}O_2$ composite wood has high efficiency and long-term mildew resistance, even if it does not rely on photocatalytic activity. The straightforward protection method is also applicable to porous materials such as bamboo and coral.

Acknowledgements

This work was supported by the Finance Science and Technology Project of Hainan Province (No. ZDYF2021SHFZ102 and ZDYF2020205), National Youth Talent Support Program, Hainan Science and Technology Major Project (No. ZDKJ2019013), National Natural Science Foundation of China (No. 51775152, 61761016, 22065012 and U1967213), National Key R&D Program of China (No. 2018YFE0103500), Start-up Research Foundation of Hainan University (No. KYQD(ZR)1911), and Project Supported by Open Project of State Key Laboratory of Marine Resource Utilization in South China Sea (Hainan University) (No. MRUKF2021025), Sichuan Provincial Youth Scientific and Technological Innovation Research Team on Ecological Adaptability of Plateau Architecture (No. 2022JDTD0008).

Conflict of Interest

There is no conflict of interest.

Supporting Information

Applicable

References

[1] S. M. Balakrishna, U. A. Lathashri, D. Sonal, U. R. Asha, B. S. Gowri, T. W. Heshan, S. Nilakshman, K. M. Prasanna, Repurposing plastic wastes in non-conventional engineered wood building bricks for constructional application – a mechanical characterization using experimental and statistical analysis, *Engineered Science*, 2022, **18**, 329–336, doi: 10.30919/es8d696.

[2] M. Auffan, W. Liu, L. Brousset, L. Scifo, A. Pariat, M. Sanles, P. Chaurand, B. Angeletti, A. Thiéry, A. Masion, J. Rose, Environmental exposure of a simulated pond ecosystem to a CuO nanoparticle-based wood stain throughout its life cycle, *Environmental Science: Nano*, 2018, **5**, 2579–2589, doi: 10.1039/c8en00712h.

[3] K. Kamau-Devers, S. A. Miller, Using a micromechanical viscoelastic creep model to capture multi-phase deterioration in bio-based wood polymer composites exposed to moisture, *Construction and Building Materials*, 2022, **314**, 125252, doi: 10.1016/j.conbuildmat.2021.125252.

[4] T. Li, M. Zhu, Z. Yang, J. Song, J. Dai, Y. Yao, W. Luo, G. Pastel, B. Yang, L. Hu, Wood composite as an energy efficient building material: guided sunlight transmittance and effective thermal insulation, *Advanced Energy Materials*, 2016, **6**, 1601122, doi: 10.1002/aenm.201601122.

[5] X. Wang, T. Zhan, Y. Liu, J. Shi, B. Pan, Y. Zhang, L. Cai, S. Q. Shi, Large-size transparent wood for energy-saving building applications, *ChemSusChem*, 2018, **11**, 4086–4093, doi: 10.1002/cssc.201801826.

[6] H. Zhang, J. Zhong, Z. Liu, J. Mai, H. Liu, X. Mai, Dyed bamboo composite materials with excellent anti-microbial corrosion, *Advanced Composites and Hybrid Materials*, 2021, **4**,

294–305, doi: 10.1007/s42114-020-00196-8.
[7] B. Andersen, J. C. Frisvad, I. Søndergaard, I. S. Rasmussen, L. S. Larsen, Associations between fungal species and water-damaged building materials, *Applied and Environmental Microbiology*, 2011, **77**, 4180–4188, doi: 10.1128/aem.02513-10.
[8] C. A. Clausen, V. Yang, Protecting wood from mould, decay, and termites with multi-component biocide systems, *International Biodeterioration & Biodegradation*, 2007, **59**, 20–24, doi: 10.1016/j.ibiod.2005.07.005.
[9] Y. M. Lee, H. Lee, Y. Jang, Y. Cho, G.-H. Kim, J.-J. Kim, Phylogenetic analysis of major molds inhabiting woods. Part 4. *Genus Alternaria, Holzforschung*, 2014, **68**, 247–251, doi: 10.1515/hf-2013-0089.
[10] J. Song, C. Chen, S. Zhu, M. Zhu, J. Dai, U. Ray, Y. Li, Y. Kuang, Y. Li, N. Quispe, Y. Yao, A. Gong, U. H. Leiste, H. A. Bruck, J. Y. Zhu, A. Vellore, H. Li, M. L. Minus, Z. Jia, A. Martini, T. Li, L. Hu, Processing bulk natural wood into a high-performance structural material, *Nature*, 2018, **554**, 224–228, doi: 10.1038/nature25476.
[11] D. Kretschmann, Velcro mechanics in wood, *Nature Materials*, 2003, **2**, 775–776, doi: 10.1038/nmat1025.
[12] J. Deng, F. Chen, G. Wang, D. Qin, X. Zhang & X. Feng, Hygrothermal aging properties, molding and abrasion resistance of bamboo keyboard, *European Journal of Wood and Wood Products*, 2014, **72**, 659–667, doi: 10.1007/s00107-014-0828-2.
[13] M. Sohail, A. Ahmad, S. A. Khan, Production of cellulases from alternaria sp. ms28 and their partial characterization, *Pakistan Journal of Botany*, 2011, **43**, 3001–3006, doi: 10.1039/b923342n.
[14] Y. Arima, H. Iwata, Effect of wettability and surface functional groups on protein adsorption and cell adhesion using well-defined mixed self-assembled monolayers, *Biomaterials*, 2007, **28**, 3074–3082, doi: 10.1016/j.biomaterials.2007.03.013.
[15] F. Chen, X. Yang, Q. Wu, Antifungal capability of TiO_2 coated film on moist wood, *Building and Environment*, 2009, **44**, 1088–1093, doi: 10.1016/j.buildenv.2008.07.018.
[16] X. Mai, J. Mai, H. Liu, Z. Liu, R. Wang, N. Wang, X. Li, J. Zhong, Q. Deng, H. Zhang, Advanced bamboo composite materials with high-efficiency and long-term anti-microbial fouling performance, *Advanced Composites and Hybrid Materials*, 2022, **5**, 864–871, doi: 10.1007/s42114-021-00380-4.
[17] X. Zhang, H. Su, Y. Zhao, T. Tan, Antimicrobial activities of hydrophilic polyurethane/titanium dioxide complex film under visible light irradiation, *Journal of Photochemistry and Photobiology A: Chemistry*, 2008, **199**, 123–129, doi: 10.1016/j.jphotochem.2008.05.002.
[18] F. Sun, B. Bao, L. Ma, A. Chen, X. Duan, Mould-resistance of bamboo treated with the compound of chitosan-copper complex and organic fungicides, *Journal of Wood Science*, 2012, **58**, 51–56, doi: 10.1007/s10086-011-1223-9.
[19] J. Han, D. Luo,Valuation on mildew-proof results of ACQ-B to bamboo, *Advanced Materials Research*, 2012, **580**, 517–520, doi: 10.4028/www.scientific.net/AMR.580.517.
[20] L. Rosu, C.-D. Varganici, F. Mustata, T. Rusu, D. Rosu, I. Rosca, N. Tudorachi, C.-A. Teacă, Enhancing the thermal and fungal resistance of wood treated with natural and synthetic derived epoxy resins, *ACS Sustainable Chemistry & Engineering*, 2018, **6**, 5470–5478, doi: 10.1021/acssuschemeng.8b00331.
[21] L. Rosu, F. Mustata, C.-D. Varganici, D. Rosu, T. Rusu, I. Rosca, Thermal behaviour and fungi resistance of composites based on wood and natural and synthetic epoxy resins cured with maleopimaric acid, *Polymer Degradation and Stability*, 2019, **160**, 148–161, doi: 10.1016/j.polymdegradstab.2018.12.022.
[22] J. Yang, Y. Chen, X. Jia, Y. Li, S. Wang, H. Song, Wood-based solar interface evaporation device with self-desalting and high antibacterial activity for efficient solar steam generation, *ACS Applied Materials & Interfaces*, 2020, **12**, 47029–47037, doi: 10.1021/acsami.0c14068.
[23] L. Huang, L. Ling, J. Su, Y. Song, Z. Wang, B. Z. Tang, P. Westerhoff, R. Ye, Laser-engineered graphene on wood enables efficient antibacterial, anti-salt-fouling, and lipophilic-matter-rejection solar evaporation, *ACS Applied Materials & Interfaces*, 2020, **12**, 51864–51872, doi: 10.1021/acsami.0c16596.
[24] G. P. Patil, S. R. Rondiya, V. S. Bagal, S. Shivhare, R. W. Cross, N. Y. Dzade, S. R. Jadkar, P. G. Chavan, Field emission characteristics of double walled TiO_2 nanotubes, *ES Materials & Manufacturing*, 2021, **13**, 76–81, doi: 10.30919/esmm5f1143.
[25] D. Pan, F. Su, H. Liu, C. Liu, A. Umar, L. Castañeda, H. Algadi, C. Wang, Z. Guo, Research progress on catalytic pyrolysis and reuse of waste plastics and petroleum sludge, *ES Materials & Manufacturing*, 2021, **11**, 3–15, doi: 10.30919/esmm5f415.
[26] M. L. de Peres, R. d. A. Delucis, S. C. Amico, D. A. Gatto, Zinc oxide nanoparticles from microwave-assisted solvothermal process: Photocatalytic performance and use for wood protection against xylophagous fungus, *Nanomaterials and Nanotechnology*, 2019, **9**, doi: 10.1177/1847980419876201.
[27] C. Liu, Y. Lin, Y. Dong, Y. Wu, Y. Bao, H. Yan, J. Ma, Fabrication and investigation on Ag nanowires/TiO_2 nanosheets/graphene hybrid nanocomposite and its water treatment performance, *Advanced Composites and Hybrid Materials*, 2020, **3**, 402–414, doi: 10.1007/s42114-020-00164-2.
[28] V. Mathur, P. K. Arya, Dynamic mechanical analysis of PVC/TiO_2 nanocomposites, *Advanced Composites and Hybrid Materials*, 2018, **1**, 741–747, doi: 10.1007/s42114-018-0051-4.
[29] D. Wiedmer, C. Cui, F. Weber, F. C. Petersen, H. Tiainen, Antibacterial surface coating for bone scaffolds based on the dark catalytic effect of titanium dioxide, *ACS Applied Materials & Interfaces*, 2018, **10**, 35784–35793, doi: 10.1021/acsami.8b12623.
[30] C. Lin, B. Liu, L. Pu, Y. Sun, Y. Xue, M. Chang, X. Li, X. Lu, R. Chen, J. Zhang, Photocatalytic oxidation removal of fluoride ion in wastewater by g-C_3N_4/TiO_2 under simulated visible light, *Advanced Composites and Hybrid Materials*, 2021, **4**, 339–349, doi: 10.1007/s42114-021-00228-x.
[31] R. Chen, J. Bao, Z. Yan, X. Huang, J. Yun, X. Zeng, J. Chen, Preparation of transparent dispersions with monodispersed ag nanoparticles for TiO_2 photoelectrode materials with excellent photovoltaic performance, *Engineered Science*, 2019, **8**, 54–65, doi: 10.30919/es8d514.

[32] S. A. Mahadik, A. Patil, H. M. Pathan, S. Salunke-Gawali, R. J. Butcher, Thionaphthoquinones as photosensitizers for TiO_2 nanorods and ZnO nanograin based dye-sensitized solar cells: effect of nanostructures on charge transport and photovoltaic performance, *Engineered Science*, 2020, **14**, 46–58, doi: 10.30919/es8d1160.
[33] G. Zhang, G. Li, J. Wang, H. Tong, J. Wang, Y. Du, S. Sun, F. Dang, 2D SnSe cathode catalyst featuring an efficient facet-dependent selective Li_2O_2 growth/decomposition for Li-oxygen batteries, *Advanced Energy Materials*, 2022, **12**, 2103910, doi: 10.1002/aenm.202103910.
[34] G. Zhang, C. Liu, L. Guo, R. Liu, L. Miao, F. Dang, Electronic "bridge" construction via Ag intercalation to diminish catalytic anisotropy for 2D tin diselenide cathode catalyst in lithium-oxygen batteries, *Advanced Energy Materials*, 2022, **12**, 2200791, doi: 10.1002/aenm.202200791.
[35] L. Guo, L. Tan, A. Xu, G. Li, G. Zhang, R. Liu, J. Wang, Y. Du, F. Dang, Highly efficient two-dimensional Ag_2Te cathode catalyst featuring a layer structure derived catalytic anisotropy in lithium-oxygen batteries, *Energy Storage Materials*, 2022, **50**, 96–104, doi: 10.1016/j.ensm.2022.05.014.
[36] H. Huang, C. Cheng, G. Zhang, L. Guo, G. Li, M. Pan, F. Dang, X. Mai, Surface phosphatization for a sawdust-derived carbon catalyst as kinetics promoter and corrosion preventer in lithium-oxygen batteries, *Advanced Functional Materials*, 2022, **32**, 2111546, doi: 10.1002/adfm.202111546.
[37] B. He, G. Li, J. Li, J. Wang, H. Tong, Y. Fan, W. Wang, S. Sun, F. Dang, $MoSe_2$ @CNT core-shell nanostructures as grain promoters featuring a direct Li_2O_2 formation/decomposition catalytic capability in lithium-oxygen batteries, *Advanced Energy Materials*, 2021, **11**, 2003263, doi: 10.1002/aenm.202003263.
[38] G. Li, N. Li, S. Peng, B. He, J. Wang, Y. Du, W. Zhang, K. Han, F. Dang, Highly efficient Nb_2C MXene cathode catalyst with uniform O-terminated surface for lithium-oxygen batteries, *Advanced Energy Materials*, 2021, **11**, 2002721, doi: 10.1002/aenm.202002721.
[39] X. Cai, T. C. Ozawa, A. Funatsu, R. Ma, Y. Ebina, T. Sasaki, Tuning the surface charge of 2D oxide nanosheets and the bulk-scale production of superlatticelike composites, *Journal of the American Chemical Society*, 2015, **137**, 2844–2847, doi: 10.1021/jacs.5b00317.
[40] X. Cai, N. Sakai, T. C. Ozawa, A. Funatsu, R. Ma, Y. Ebina, T. Sasaki, Efficient photoinduced charge accumulation in reduced graphene oxide coupled with titania nanosheets to show highly enhanced and persistent conductance, *ACS Applied Materials & Interfaces*, 2015, **7**, 11436–11443, doi: 10.1021/acsami.5b02107.
[41] X. Cai, L. Yin, N. Sakai, D. Liu, C. Teng, Y. Ebina, R. Ma, T. Sasaki, Photocharge trapping in two-sheet reduced graphene oxide-$Ti_{0.87}O_2$ heterostructures and their photoreduction and photomemory applications, *ACS Applied Nano Materials*, 2019, **2**, 6378–6386, doi: 10.1021/acsanm.9b01348.
[42] M. Osada, Y. Ebina, H. Funakubo, S. Yokoyama, T. Kiguchi, K. Takada, T. Sasaki, High-κ dielectric nanofilms fabricated from titania nanosheets, *Advanced Materials*, 2006, **18**, 1023-1027, doi: 10.1002/adma.200501224.
[43] K. Behm, E. Fazekas, M. J. Paterson, F. Vilela, R. D. McIntosh, Discrete Ti–O–Ti complexes: visible-light-activated, homogeneous alternative to TiO_2 photosensitisers, *Chemistry - A European Journal*, 2020, **26**, 9486–9494, doi: 10.1002/chem.202001678.

